ELSEVIER

Aerosol Science 35 (2004) 909–922

Journal of
Aerosol Science

www.elsevier.com/locate/jaerosci

Technical note

A generalised method for the extraction of chemically resolved mass spectra from Aerodyne aerosol mass spectrometer data

James D. Allan[a,*], Alice E. Delia[b], Hugh Coe[a], Keith N. Bower[a], M. Rami Alfarra[a,1], Jose L. Jimenez[c], Ann M. Middlebrook[d], Frank Drewnick[e], Timothy B. Onasch[f], Manjula R. Canagaratna[f], John T. Jayne[f], Douglas R. Worsnop[f]

[a] *Department of Physics, University of Manchester Institute of Science and Technology (UMIST), P.O. Box 88, Manchester M60 1QD, UK*

[b] *Program in Atmospheric and Oceanic Science, University of Colorado, Stadium 255, Boulder, CO 80309-0311, USA*

[c] *CIRES & Department of Chemistry, University of Colorado, UCB 216, Boulder, CO 80309-0216, USA*

[d] *NOAA Aeronomy Laboratory, 325 Broadway, R/AL7, Boulder, CO 80305-3328, USA*

[e] *Department of Cloud Physics and Chemistry, Max Planck Institute for Chemistry, Joh.-J.-Becher-Weg 27, Universitätscampus, D-55128 Mainz, Germany*

[f] *Aerodyne Research Inc., 45 Manning Road, Billerica, MA 01821-3976, USA*

Received 15 October 2003; received in revised form 13 February 2004; accepted 18 February 2004

Abstract

A generalised method for the deconvolution of mass spectral data from the aerodyne aerosol mass spectrometer (AMS) is presented. In this instrument, the sampled ensemble of gas and non-refractory particle phase materials interfere with each other in the mass spectra and the data must be systematically analyzed to generate meaningful, quantitative and chemically resolved results. The method presented here is designed to arithmetically separate the raw data into partial mass spectra for distinct chemical species. This technique was developed as part of the AMS analysis tools introduced by Allan et al. (J. Geophys. Res. Atmos. 108 (2003) 4090) and is in use by most groups within the AMS users community. This technique employs a user-definable 'fragmentation table' for each chemical species or group of species, and examples of some tables designed for the interpretation of field data are given. The ongoing work being performed to develop and validate the tables will be presented in future publications.

Keywords: Aerosol mass spectrometry; Data analysis; Inversion techniques

* Corresponding author. Tel.: +161-236-3311x62490; fax: +44-161-200-3951.
E-mail address: james.allan@physics.org (J.D. Allan).

[1] During this work, was at the department of chemical engineering, UMIST.

0021-8502/$ - see front matter © 2004 Elsevier Ltd. All rights reserved.
doi:10.1016/j.jaerosci.2004.02.007

1. Introduction

The aerodyne aerosol mass spectrometer (AMS) is a powerful and versatile instrument, capable of delivering online quantitative data on mass concentrations and size distributions of fine particulate components (Jayne et al., 2000). Its basic principle of operation is to impact a focused particle beam onto a porous tungsten surface (the vaporiser, typically heated to 600°C), under ultra-high vacuum, flash vaporise the non-refractory components of the particles, ionise the vapour using 70 eV electron impact (EI) ionisation and analyse the resultant ions using a quadrupole mass spectrometer with unit mass-to-charge (m/z) resolution. The term 'non-refractory' (NR) is defined operationally as those species that evaporate rapidly (<5 s) at the AMS temperature and vacuum conditions.

The instrument is typically alternated between two modes of operation; mass spectrum (MS) mode and time-of-flight (TOF) mode (Jimenez et al., 2003). In MS mode, an average mass spectrum (typically m/z 1–300) representing the NR components of the sampled particles is reported for a fixed sampling interval (e.g. 5 min). Any signals due to the presence of background gases in the detection region are evaluated by using a mechanical chopper to block the beam and the measured background spectrum is mathematically subtracted from that of the sample. This 'ensemble' mass spectrum also contains signal from the sampled gas-phase species. The aerodynamic lens and differential pumping system of the AMS reduces the gas-phase signal (relative to the particles) by a factor of 10^7. However, the concentrations of the major air species are much larger than those of the particles (e.g. ≈ 950 g m^{-3} for N_2 compared to total aerosol concentrations of 1–50 μg m^{-3}), meaning gas-phase species account for most of the signal at certain m/z peaks. During atmospheric sampling, these are normally m/z 18 (H_2O^+), 28 (N_2^+), 32 (O_2^+) and 40 (Ar^+), with additional peaks due to fragments, isotopes and doubly charged ions. A signal from gas-phase CO_2 can be detected at m/z 44 but other gas phase species (e.g. methane) with mixing ratios less than about 10 ppm produce signals below the detection limit of the current AMS configurations.

The separation of the particle vaporisation and ionisation processes means that the mass spectra produced for different chemical species, once vaporised, are clearly defined, quantitative, reproducible and independent of the other species in the detection region. Laboratory characterisation and validation work has shown that when particles of single chemical species are generated and introduced into the instrument, distinctive mass spectra can be obtained from the vaporised particles (Jayne et al., 2000; Jimenez et al., 2003). Furthermore, these mass spectra are comparable to those held on the National Institute of Standards and Technology (NIST) database (Linstrom & Mallard, 2003), meaning that the instrument's response to a given chemical species can be predicted based on existing literature regarding standard 70 eV EI quadrupole mass spectrometry.

There are certain cases where discrepancies exist between the AMS and the NIST database, due to the fact that the particulate species are vaporised at high temperature (typically 600°C) prior to detection. For instance, when vaporising ammonium sulphate ($(NH_4)_2SO_4$) particles, the vapours generated and detected are molecular NH_3, H_2SO_4, SO_3 and H_2O. Also, some of the more complex molecules may undergo additional fragmentation due to the heat transferred from the vaporiser. In these cases, the lower m/z peaks in the mass spectrum are enhanced relative to the corresponding NIST spectrum, while the higher m/z peaks show a reduction. Also, di- and poly-carboxylic acids are known to undergo decarboxylation, producing significant signals at m/z 18 (H_2O^+) and 44 (CO_2^+), which are not present in the corresponding spectra held on the NIST database. However,

none of these issues affect the instrument's quantitative capability, providing that all of the resultant fragments are accounted for.

While the instrument is proven to be capable of delivering quantitative data on single chemical species introduced into the instrument (Jayne et al., 2000), it becomes difficult when many species are sampled simultaneously, as is routinely the case for ambient atmospheric data. The different species interfere with one another in the mass spectrum, making it difficult to identify and quantify specific aerosol components. This has necessitated the development of data analysis techniques that can accurately separate the various contributions, a necessary step in producing useful and reliable data. A generalised and flexible method of performing this is presented in this paper.

2. Existing techniques

Before exploring the new techniques, it is important to put them in the context of the existing methods. The basic underlying equation for converting a detected ion rate (I, in counts per second or Hz) reported at a specific mass to charge ratio (m/z), to a mass concentration (C, in $\mu g\ m^{-3}$) was presented by Jimenez et al. (2003) as follows:

$$C = 10^{12}\,\frac{1}{\mathrm{IE}}\,\frac{1}{Q}\,\frac{\mathrm{MW}}{N_A}\,I, \tag{1}$$

where MW is the molecular weight of the species in question in $g\ mol^{-1}$, N_A Avagadro's number, Q the volumetric sample flow rate into the instrument in $cm^3\ s^{-1}$ and IE the ionisation efficiency, a dimensionless quantity equalling the number of ions detected per molecule of the parent species, which is typically of the order of 10^{-6}. Note that the latter includes not only the probability of a desorbed molecule becoming ionised, but also the transmission efficiency of the mass spectrometer and the detection efficiency of the electron multiplier. This is specific to the chemical species and the ions being studied. Also note that the probability of a particle becoming successfully introduced into the instrument and vaporised (known as the particle collection efficiency or CE) is not included, as this publication only considers instrument behaviour after particle vaporisation. However, the CE must be taken account of in real world applications and is considered in all current fieldwork analyses (e.g. Alfarra et al., in press). The factor of 10^{12} is included to convert from $g\ cm^{-3}$ to $\mu g\ m^{-3}$.

Molecules of most species undergo fragmentation during the electron impact ionisation process. For example, there are two major nitrate peaks in the mass spectrum of ammonium nitrate aerosol at m/z 30 (NO^+) and m/z 46 (NO_2^+). To measure the total mass concentration of nitrate (NO_3) using the method described by Allan et al. (2003a), both fragments must be summed, as follows:

$$C_{NO_3} = 10^{12}\frac{\mathrm{MW}_{NO_3}}{\mathrm{IE}_{NO_3}\,Q\,N_A}\,(I_{30} + I_{46}). \tag{2}$$

This approach can be easily applied to ambient data for species such as nitrate and sulphate, where their major peaks are normally distinct in the ensemble mass spectrum and contributions from interfering species (e.g. organics) are low. However, the technique of simply summing the ion rates for individual m/z channels in the ensemble mass spectrum is not sufficient for most species. For example, the calculation of ammonium concentrations is not possible using this technique alone and the ability to provide this measurement is greatly desired from a scientific point of view.

Through laboratory studies using particles generated from an aqueous solution, it is known that particulate ammonium vaporises as ammonia (NH_3) and fragments under electron impact ionization to produce three major ions: m/z 15 (NH^+), 16 (NH_2^+) and 17 (NH_3^+). The relative sizes of these peaks in the mass spectrum have been found to be independent of the anion used in the solution, which is due to the vaporisation and ionisation processes being decoupled. However, it is not possible to use these signals from the ensemble mass spectrum directly, as they all receive significant interferences from other species in the ensemble mass spectrum, most notably the $^{15}N^+$, CH_3^+, O^+, O_2^{2+} and OH^+ ions.

In practice, m/z 15 is often ruled out as a useful channel for the calculation of ammonium concentrations because it is a minor peak in the ammonia mass spectrum (around 10% of the size of the m/z 16 peak), with a consequently low signal-to-noise ratio. Also, it is difficult to determine quantitatively how much of the signal present is made up of CH_3^+ ions from certain organic species. Instead, it was found that it is possible to use the ammonia signals at m/z 16 and 17 for the calculation of ammonium concentrations, provided that the fractions of the signals due to interfering chemicals are predicted correctly. The first application of this specific technique will be presented in Delia et al. (in preparation).

The O^+ and O_2^{2+} contributions originating from gas-phase oxygen can be predicted based on the signals from other major gas phase signals, as the ratio between these should be invariant as long as the ionisation, ion extraction and mass analysis conditions do not change. It has been found that using the signal at m/z 14 (N^+ and N_2^{2+}) multiplied by a factor is the least susceptible to artefacts created by minor interferences by other species and changes in the quadrupole or ioniser performance. The EI fragmentation of water also produces large numbers of O^+ ions, but these can be predicted based on the signal at m/z 18, which is almost entirely due to H_2O^+ ions. The fragmentation pattern of water molecules has been observed to be independent of their source, whether they are from water vapour in the air beam, particle phase water in aqueous particles or from thermal decomposition of other chemical species on the heated surface. Similarly, the contribution of the OH^+ ion from water to the signal at m/z 17 can also be predicted based on the signal at m/z 18.

To summarise, the work by Delia et al. (in preparation) concluded that the signals due to vaporised ammonia at m/z 16 and 17 ($I_{NH_4,16}$ and $I_{NH_4,17}$) can be calculated from the raw mass spectrum as follows:

$$I_{NH_4,16} = I_{16} - a_1 I_{14} - a_2 I_{18},$$
$$I_{NH_4,17} = I_{17} - a_3 I_{14} - a_4 I_{18}, \quad (3)$$

where a_1, a_2, a_3 and a_4 are multipliers whose values are based on the measured fragmentation patterns of air and water. The subtraction applied to $I_{NH_4,17}$ based on I_{14} is due to the $^{17}O^+$ and $^{16}O^{18}O^{2+}$ ions. As these isotopes make up less than 0.3% of the total oxygen, a_3 will be small. The ammonium signal at m/z 15 ($I_{NH_4,15}$) is based on $I_{NH_4,16}$, as follows:

$$I_{NH_4,15} = a_5 I_{NH_4,16} = a_5 I_{16} - a_1 a_5 I_{14} - a_2 a_5 I_{18}, \quad (4)$$

where a_5 is based on laboratory measured fragmentation patterns of vaporised ammonia. These three calculated ammonia signals can then be summed and converted to a mass concentration of ammonium in a similar manner to Eq. (2). When using this technique, the quantitative capability of the AMS at a given m/z channel is limited by two main factors; the signal to noise ratio at that

channel due to instrument background levels, electronic noise and the signal intensity being measured (Allan et al., 2003a) and interference between multiple species when one species' abundance is significantly greater than that of another.

3. The new methodology

While the above technique has been used to generate ammonium mass concentrations effectively, it highlights a more general problem of interferences within the mass spectra, which is applicable to all species. Previous work that used the summation technique of Allan et al. (2003a) could only reliably calculate mass concentrations for sulphate and nitrate when their corresponding peaks were sufficiently distinct. Additionally, the calculated organic data were frequently subject to artefacts caused by minor inorganic peaks that were not accounted for (e.g. $^{34}SO^{+}$). From the ammonium exercise, it also became apparent that the study of species with even smaller contributions to the overall mass spectrum (e.g. chloride) would be more difficult still.

For these reasons, a new generalised method was developed with a view to being universally applied to all species as part of the standard analysis tools. The underlying approach is to extract a 'partial' mass spectrum corresponding to a particular chemical species from the ensemble mass spectrum using known relationships between the peaks of all of the species involved. For example, in the case of ammonium described above, the magnitude of the signals at m/z 15, 16 and 17 due to vaporised ammonia is calculated based on the signals at m/z 14, 16, 17 and 18 in the ensemble spectrum. For the purposes of the general analysis, the following approach was used to process the ensemble mass spectrum:

$$\vec{I}_{\mathrm{s}} = \mathbf{M}_{\mathrm{s}}\vec{I}_{\mathrm{en}}, \tag{5}$$

where $\vec{I}_{\mathrm{s}}$ is the partial mass spectrum due to species s, $\vec{I}_{\mathrm{en}}$ the ensemble mass spectrum retrieved from the instrument and $\mathbf{M}_{\mathrm{s}}$ a square conversion matrix specific to the species. The recorded mass spectrum and the deconvolved partial mass spectra are treated as vectors of ion rates with dimensions equalling the number of discrete m/z channels scanned, e.g. a 300 dimension vector if the m/z range 1–300 was scanned during operation. Using this approach, any single peak intensity in any species' partial mass spectrum can be estimated as a linear combination of the peaks in the ensemble mass spectrum. The conversion matrices are generated using laboratory derived fragmentation ratios of all the species and knowledge of isotopic ratios and instrument performance. In practice, the contributions from the majority of channels in the ensemble spectrum to a given channel in a species' partial spectrum will be insignificant and so the conversion matrix, $\mathbf{M}_{\mathrm{s}}$, will be sparse and a non-circular solution can be found.

When calculating the total mass concentrations of particular chemicals, the total ion rates are calculated by summing all of the peaks in their partial mass spectrum, giving the following generalised formula:

$$C_{\mathrm{s}} = 10^{12}\,\frac{\mathrm{MW_s}}{\mathrm{IE_s}\,Q\,N_{\mathrm{A}}}\sum_{\mathrm{all}\ i} I_{\mathrm{s},i}. \tag{6}$$

It is impractical to experimentally determine specific values of IE for each species and each experiment. Normally, only $\mathrm{IE}_{\mathrm{NO_3}}$ is determined during routine calibration. $\mathrm{IE_s}/\mathrm{IE}_{\mathrm{NO_3}}$ should be

constant across experiments if the ionisation conditions are the same, because electron ionisation is a physical process involving only the interaction of 70 eV electrons with isolated molecules under vacuum (Jimenez et al., 2003). For these reasons, relative ionisation efficiencies (RIE) are used, as first introduced by Alfarra et al. (in press). These are simply the ratio of the ionisation efficiency of a species to that of nitrate and generate the following formula:

$$C_s = 10^{12} \frac{MW_{NO_3}}{RIE_s \, IE_{NO_3} Q N_A} \sum_{\text{all } i} I_{s,i}. \tag{7}$$

4. Fragmentation tables

In order to generate the conversion matrices ($\mathbf{M}_s$), a system of fragmentation tables has been developed. Operationally, each table represents a different chemical species, with each row being an m/z in that species' partial mass spectrum. Within the table, the user defines which peaks exist in each species' partial mass spectrum and their dependencies on other peaks in their own mass spectrum, the mass spectra of other species or the ensemble mass spectrum.

Examples of such tables, formatted as used in the software, are shown in Tables 1–3. The species-specific column names are preceded with 'frag_' for identification purposes. Each entry consists of a comma-separated list of the components that must be summed to obtain the value of that channel in the species' partial mass spectrum. These components can be peaks in the ensemble mass spectrum, which in this note are denoted by an integer number in square brackets (in the actual software, the square brackets are omitted, but are included here for clarity). Alternatively, a cross-reference to another entry in the fragmentation tables can be given, which is denoted by the name of the table in question followed by a number in square brackets, identifying the referenced m/z in the table. The references can also be specified as having a negative contribution (to remove interferences) by the inclusion of a minus sign, or can include multipliers if a fractional contribution is required.

The development of extensive and reliable fragment tables, applicable to all instruments, is the result of ongoing collaborative work by several groups within the AMS community. The examples shown in this note are part of the tables used for analysing ambient AMS data, current at the time of submission, although these are continually being developed and are frequently changed to suit specific laboratory or field applications and many different versions are already in existence. Some other versions of these tables can be obtained from the website given at the end of this paper. The function of this publication is not to validate the contents of the tables, rather to present the underlying methodology, give examples and provide a basis for future publications that will perform the former function.

There are certain peaks that arise due to minor isotopes, for example, the peak at m/z 29 due to $^{15}N^{14}N^{+}$. These peaks are denoted by an [a] flag in the tables and the ratios were predicted based on the IUPAC recommended isotopic abundances (Coplen et al., 2002; De Laeter et al., 2003). Patterns due to molecular fragmentation for the main inorganic species were obtained by analysing laboratory-generated single component particles and are denoted by a [b] flag. Detailed information on this work will be presented in future publications, but typical experiments used carrier gases of controlled compositions, for example pure argon, to minimise the interferences to the particle-phase

Table 1
The fragmentation tables for the chemical components of air (frag_air), particulate nitrate (frag_NO_3), potassium (frag_K) and chloride (frag_Cl)

m/z	frag_air	frag_nitrate	frag_K	frag_chloride
14	[14], −frag_nitrate[14]	0.04*frag_nitrate[30][b], 0.04*frag_nitrate[46][b]		
15	0.00368*frag_air[14][a]			
16	Frag_O16[16], frag_RH[16]			
17	0.000391*frag_O16[16][a], frag_RH[17]			
18	0.002*frag_O16[16][a], frag_RH[18]			
19	frag_RH[19]			
20	[20], −frag_organic[20], −frag_sulphate[20], −frag_water[20]			
...				
28	[28]			
29	0.00736*frag_air[28][a]			
30	0.0000136*frag_air[28][a]	[30], −frag_air[30], −frag_organic[30]		
31		0.00405*frag_nitrate[30][a]		
32	[32], −frag_sulphate[32], −frag_nitrate[32]	0.002*frag_nitrate[30][a]		
33	0.000763*frag_air[32][a]			
34	0.00402*frag_air[32][a]			
35				[35]
36	0.00338*frag_air[40][a]			[36], −frag_air[36]
37				0.323*frag_chloride[35][a]
38	0.000633*frag_air[40][a]			0.323*frag_chloride[36][a]
39			[39]	
40	[40]			
41			0.0722*frag_K[39][a]	
...				
44	0.000734*frag_air[28][b]			
45				
46		[46]		
47		0.00443*frag_nitrate[46][a]		
48		0.004*frag_nitrate[46][a]		
...				
63		0.003*frag_nitrate[30][b], 0.002*frag_nitrate[46][b]		

Contributions marked with an [a] use multipliers based on predicted contributions from common isotopes. Those marked with a [b] are based on the analysis of laboratory and field studies, which will be presented in future publications. The entry at frag_air[44] is an estimate of the gas-phase CO_2 contribution to the mass spectrum. This may require tweaking depending on the ambient concentration during an experiment. Omitted rows are blank. Note that all contributions from the ^{37}Cl isotope are calculated based on signals due to ^{35}Cl.

signals. This type of analysis now permits the use of more peaks within a species' mass spectrum. For instance, rather than the two *m/z* signal contributions used in Eq. (2), the table for nitrate actually contains eight contributions from vaporised nitric acid, which include the parent ion at *m/z* 63, minor

Table 2
The fragmentation tables for gas phase water (frag_RH), the $^{16}O^+$ and $^{16}O_2^{2+}$ fragments due to gas phase oxygen (frag_O16), particulate water (frag_water) and ammonium ($frag\_NH_4$)

m/z	frag_RH	frag_O16	frag_water	$frag\_NH_4$
15				0.1*frag_NH_4[16][b]
16	0.04*frag_RH[18][b]	0.353*frag_air[14][b]	0.04*frag_water[18][b]	[16], −frag_water[16], −frag_air[16], −frag_sulphate[16], −frag_organic[16]
17	0.25*frag_RH[18][b]		0.25*frag_water[18][b]	[17], −frag_water[17], −frag_air[17], −frag_sulphate[17], −frag_organic[17]
18	0.01*frag_air[28][b]		[18], −frag_air[18], −frag_sulphate[18], −frag_organic[18]	
19	0.000691*frag_RH[18][a], 0.002*frag_RH[17][a]		0.000691*frag_water[18][a], 0.002*frag_water[17][a]	
20	0.002*frag_RH[18][a]		0.002*frag_water[18][a]	

The relative contribution to the gas phase from water vapour is typically variable in time and to be completely thorough, should be accounted for by adjusting the multiplier in the frag_RH[18] entry. However, any inaccuracy in this number will only affect the ability to quantitatively distinguish water vapour from particulate water, which is not required in most applications. The ratio governing the $^{16}O^+$ and $^{16}O_2^{2+}$ peak is variable between instruments and configurations and has to be set correctly in order to be able to calculate ammonium concentrations correctly.

isotope ions at *m/z* 31, 32, 47, and 48 and the N^+ fragment at *m/z* 14. Also, as mentioned earlier, ammonium sulphate vaporises as NH_3, H_2O, SO_3 and H_2SO_4. The amount of ammonium and water present in the particles can shift the vaporisation equilibrium between H_2SO_4 and SO_3 plus H_2O, therefore it is necessary to handle these separately, as they have different individual mass spectra. As stated before, these phenomena are currently under investigation and details will be presented in future publications.

There are certain aspects of the fragmentation tables that are known to change between instruments, instrument configurations and even deployments. For instance, the value of the O^+ and O_2^{2+} to N^+ and N_2^{2+} ratio mentioned above is known to vary slightly depending on the precise set-up of the ioniser and quadrupole. Therefore, this value must be carefully set when analysing a dataset if reliable ammonium concentrations are to be calculated, as the O^+ and O_2^{2+} signal is typically large compared to that of NH_2^+. Also, the values of certain quantities are dependent on the sampling environment, for example the contribution of gas-phase CO_2 to the *m/z* 44 peak. This contribution must be set by the user and in certain circumstances, for example when sampling low organic concentrations or when sampling combustion sources directly, may have to be time-dependent. These values can be obtained by analysing the mass spectra of filtered air, which should be taken routinely during sampling. If the calculated particle signals at *m/z* 16 and 44 are non-zero, the values in the fragmentation tables are altered accordingly, as the only significant signals observed through the filter are from the gas phase.

Table 3
The fragmentation tables for total sulphate (frag_sulphate), sulphur trioxide (frag_SO_3), sulphuric acid (frag_H_2SO_4) and organics (frag_organic)

m/z	frag_sulphate	frag_H_2SO_4	frag_SO_3	frag_organic
12				[12]
13				[13]
14				
15				[15], −frag_NH_4[15], −frag_air[15]
16	frag_SO_3[16]		0.04*frag_SO_3[18][b]	0.04*frag_organic[18][b]
17	frag_SO_3[17]		0.25*frag_SO_3[18][b]	0.25*frag_organic[18][b]
18	frag_SO_3[18]		0.67*frag_SO_3[64][b], 0.67*frag_SO_3[48][b]	1*frag_organic[44][b]
19	frag_SO_3[19]		0.000691*frag_SO_3[18][a], 0.002*frag_SO_3[17][a]	0.000691*frag_organic[18][a], 0.002*frag_organic[17][a]
20	frag_SO_3[20]		0.002*frag_SO_3[18][a]	0.002*frag_organic[18][a]
...				
24	frag_SO_3[24], frag_H_2SO_4[24]	0.005*frag_H_2SO_4[48][b]	0.005*frag_SO_3[48][b]	[24], −frag_sulphate[24]
25				[25]
26				[26]
27				[27]
28				
29				[29], −frag_air[29]
30				0.022*frag_organic[29][a]
31				
32	frag_SO_3[32], frag_H_2SO_4[32]	0.068*frag_H_2SO_4[81][b], 0.068*frag_H_2SO_4[98][b]	0.21*frag_SO_3[48][b], 0.21*frag_SO_3[64][b]	
33	frag_SO_3[33], frag_H_2SO_4[33]	0.0079*frag_H_2SO_4[32][a]	0.0079*frag_SO_3[32][a]	
34	frag_SO_3[34], frag_H_2SO_4[34]	0.044*frag_H_2SO_4[32][a]	0.044*frag_SO_3[32][a]	
...				
37				[37], −frag_chloride[37]
38				[38], −frag_chloride[38], −frag_air[38]
...				
41				[41], −frag_K[41]
42				[42]
43				[43]
44				[44], −frag_air[44]
45				[45]
...				
48	frag_SO_3[48], frag_H_2SO_4[48]	0.465*frag_H_2SO_4[81][b], 0.465*frag_H_2SO_4[98][b]	[48], −frag_organic[48], −frag_nitrate[48], −frag_H_2SO_4[48]	0.5*frag_organic[62]
49	frag_SO_3[49], frag_H_2SO_4[49]	0.00829*frag_H_2SO_4[48][a], 0.015*frag_H_2SO_4[81][b], 0.015*frag_H_2SO_4[98][b]	0.00829*frag_SO_3[48][a]	[49], −frag_sulphate[49]

Table 3 (*continued*)

m/z	frag_sulphate	frag_H_2SO_4	frag_SO_3	frag_organic
50	frag_SO_3[50], frag_H_2SO_4[50]	0.0462* frag_H_2SO_4[48][a]	0.0462* frag_SO_3[48][a]	[50], −frag_sulphate[50]
51				[51]
52	frag_SO_3[52], frag_H_2SO_4[52]	0.000299* frag_H_2SO_4[48][a]	0.000299* frag_SO_3[48][a]	[52], −frag_sulphate[52]
53				[53]
54				[54]
55				[55]
56				[56]
57				[57]
58				[58]
59				[59]
60				[60]
61				[61]
62				[62]
63				[63], −frag_nitrate[63]
64	Frag_SO_3[64], frag_H_2SO_4[64]	0.465* frag_H_2SO_4[81][b], 0.465* frag_H_2SO_4[98][b]	[64], −frag_organic[64], −frag_H_2SO_4[64]	0.5* frag_organic[50][b], 0.5* frag_organic[78][b]
65	Frag_SO_3[65], frag_H_2SO_4[65]	[65], −frag_organic[65], −frag_SO_3[65]	0.00868* frag_SO_3[64][a]	0.5* frag_organic[51][b], 0.5* frag_organic[79][b]
66	Frag_SO_3[66], frag_H_2SO_4[66]	0.0482* frag_H_2SO_4[64][a], 0.004* frag_H_2SO_4[81][b], 0.004* frag_H_2SO_4[98][b]	0.0482* frag_SO_3[64][a]	[66], −frag_sulphate[66]
67				[67]
68				[68]
69				[69]
70				[70]
71				[71]
72				[72]
73				[73]
74				[74]
75				[75]
76				[76]
77				[77]
78				[78]
79				[79]
80	Frag_SO_3[80], frag_H_2SO_4[80]	0.75*[80][b], −0.75* frag_organic[80][b]	0.25*[80][b], −0.25* frag_organic[80][b]	0.75* frag_organic[94][b]
81	Frag_H_2SO_4[81]	[81], −frag_organic[81]		0.5* frag_organic[67][b], 0.5* frag_organic[95][b]
82	Frag_SO_3[82], frag_H_2SO_4[82]	0.0502* frag_H_2SO_4[80][a], 0.00922* frag_H_2SO_4[81][a]	0.0502* frag_SO_3[80][a]	[82], −frag_sulphate[82]
83	Frag_H_2SO_4[83]	0.0502* frag_H_2SO_4[81][a]		[83], −frag_sulphate[83]
84	Frag_SO_3[84], frag_H_2SO_4[84]	0.000488* frag_H_2SO_4[80][a]	0.000488* frag_SO_3[80][a]	[84], −frag_sulphate[84]
85	Frag_H_2SO_4[85]	0.000488* frag_H_2SO_4[81][a]		[85], −frag_sulphate[85]
86				[86]
87				[87]

Table 3 (*continued*)

m/z	frag_sulphate	frag_H_2SO_4	frag_SO_3	frag_organic
88				[88]
89				[89]
90				[90]
91				[91]
92				[92]
93				[93]
94				[94]
95				[95]
96				[96]
97				[97]
98	Frag_H_2SO_4[98]	[98], −frag_organic[98]		0.5*frag_organic[84][b], 0.5*frag_organic[112][b]
99	Frag_H_2SO_4[99]	0.00976*frag_H_2SO_4[98][a]		[99], −frag_sulphate[99]
100	Frag_H_2SO_4[100]	0.0522*frag_H_2SO_4[98][a]		[100], −frag_sulphate[100]
101				[101]
102	Frag_H_2SO_4[102]	0.00059*frag_H_2SO_4[98][a]		[102], −frag_sulphate[102]

When sulphate compounds are vaporised, H_2SO_4, SO_3 and H_2O are produced in the detection region in varying proportions, depending on the particle composition. Note that the H_2O contribution from the vaporisation of H_2SO_4 is included in frag_SO_3, as it is formed in equal molar quantities with the SO_3. The sulphate mass spectrum is taken to be the sum of these spectra. Any peaks in the ensemble mass spectrum of an m/z greater than 102 are assumed to be organic during normal ambient sampling. The exceptions are m/z 149, 180, 182, 183 and 184, as these channels tend to have high background levels in the instrument and would therefore introduce too much inherent noise to the summed signal. However, as the fraction of the total organic mass residing in the $m/z > 100$ regime is typically small, these omissions do not significantly affect the overall calculation.

The organic fragmentation table is based on the assumption that any detected matter that cannot be accounted for by known inorganic components must be organic, the same assumption that was used by Allan et al. (2003a). There are certain peaks in the ensemble mass spectrum that contain both inorganic and organic mass signals. In most cases, a minor inorganic contribution is calculated based on larger peaks in that species' spectrum and laboratory measured fragmentation patterns. Where this is not possible, for example at m/z 64, the organic contribution is instead based on the other signals in the organic mass spectrum. In this case, the numerical average of the signals at m/z 50 and 78 are used, as these correspond to the addition and subtraction of a CH_2 group from hydrocarbon fragments; long chained saturated hydrocarbons will fragment under standard 70 eV electron impact ionization by loss of C_nH_{2n+1} alkyl groups (McLafferty & Turecek, 1993, Chapter 5). While this is only an approximation, it has been found to be fairly robust during episodes where the high m/z organic component of ambient aerosol is composed of long chained, saturated hydrocarbons such as lubricating oils, which is typical of urban environments (e.g. Allan et al., 2003b).

The analysis software performs the conversion from a fragmentation table column to a matrix in two stages. The first stage is to iteratively evaluate all the cross-references until only references to m/z channels in the ensemble mass spectrum remain. This generates an intermediate table. The second stage is to generate the matrix from this new table, and an example is shown in Table 4, which is the conversion matrix for ammonium ($\mathbf{M}_{NH_4}$). The ith row of a matrix corresponds to the ith m/z channel of the species' partial mass spectrum, or the ith row of the fragmentation table.

Table 4
Part of the conversion matrix used for the extraction of the ammonium mass spectrum ($\mathbf{M}_{NH_4}$)

	14	15	16	17	18	···	29	30	···	46
15	−3.53e − 02	0	0.1	0	−4.00e − 03		−3.11e − 05	1.41e − 03		1.41e − 03
16	−3.53e − 01	0	1	0	−4.00e − 02		−3.10e − 04	1.41e − 02		1.41e − 02
17	3.85e − 05	0	0	1	−2.50e − 01		3.39e − 08	−1.54e − 06		−1.54e − 06

Values not shown are zero or less than 10^{-5} in magnitude, i.e. contribute less than 10 parts per million to the total. Data are shown to 3 significant figures for clarity.

The *j*th column of the matrix corresponds to the *j*th *m/z* channel of the ensemble mass spectrum. The individual contributions (i.e. the fully evaluated multipliers) specified in the intermediate table are added to the matrix according to their row in the table and column corresponding to the *m/z* channel in the ensemble mass spectrum that each entry refers to. As mentioned earlier, the matrices generated using this technique tend to be very sparse, so only part of it is shown for clarity. The values not shown in this example are zero or otherwise less than 10^{-5} in magnitude.

The matrix contains unity values at [16][16] and [17][17], which shows that the calculated values of the ammonium partial mass spectrum at *m/z* 16 and 17 include those of the ensemble mass spectrum. The various negative values in columns 14 and 18 show that subtractions are made based on the signals at *m/z* 14 and 18. These are, respectively, manifestations of the oxygen (O^+ and O_2^{2+}) and water (O^+ and OH^+) fragment subtractions mentioned in the introduction and detailed in Eq. (3). Note the exception is the value at row 17, column 14, which is slightly positive. Eq. (3) deals with a minor subtraction at *m/z* 17 due to the $^{17}O^+$ and $^{16}O^{18}O^{2+}$ ions but an additional correction is also made to the water signal at *m/z* 18 due to the $^{18}O^+$ ion from gas phase oxygen, which manifests as a net positive influence on 17 that largely cancels out the former correction.

The zero value at [15][15] shows that there is no contribution to the calculated value at *m/z* 15 from the corresponding signal in the ensemble mass spectrum; instead, it is based on the signals at *m/z* 14, 16 and 18, in the same way as Eq. (4). The entries at columns 30 and 46 come about because the aforementioned subtraction of the O^+ and O_2^{2+} signal is based on the N^+ and N_2^{2+} signal from air, which in turn must include a correction due to the N^+ fragment from nitrate (NO_3) in the particle phase. This correction is based on the signals at *m/z* 30 (NO^+) and 46 (NO_2^+). *m/z* 30 also contains a minor contribution from organic signal fragments containing a single ^{13}C isotope, which is predicted based on the signal at *m/z* 29, hence the small dependency there. There are other dependencies elsewhere in the matrix, but these are smaller still. While the extra accuracy achieved through the smaller of these corrections is probably small compared to other errors or uncertainties associated with the instrument, they do demonstrate the thoroughness of the technique.

5. Summary

This technical note presents a new generalised technique for separating the ensemble mass spectra obtained by the Aerodyne Aerosol Mass Spectrometer into chemically resolved partial mass spectra, which has been integrated into the standard AMS analysis routines used by the AMS users

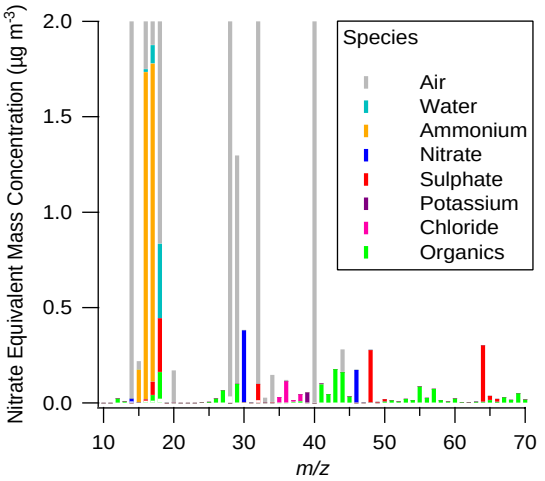

Fig. 1. An example of a chemically resolved mass spectrum that can be obtained using the techniques presented. The term 'nitrate equivalent mass' refers to the fact that the values reported have yet to have their species-specific relative ionisation efficiencies (RIE_s, Eq. (7)) applied, as this would make a like-for-like comparison impossible. Most of the air peaks are off scale. Signals below the detection limits are blanked out, as described by Allan et al. (2003a).

community. These new techniques employ matrix arithmetic that allows interferences between species to be accounted for explicitly and completely. User-defined fragmentation tables for the individual species are employed and while this paper does not attempt to validate the tables themselves, the underlying methodology provides the basis for the future publications.

As well as being able to calculate mass concentrations, another advantage of this approach is that parts of peaks within graphed mass spectra can be coloured according to their chemical sources, facilitating data interpretation. An example of this is shown in Fig. 1, which uses data from sampling ambient air in Manchester during January 2002 (Allan et al., 2003b) and the example tables presented. As a diagnostic tool, the peak ratios in the partial mass spectra can be compared with expected values and the partial mass spectra summed and compared with the ensemble mass spectra they are derived from. Any inconsistencies are normally indicative of either one or more incorrectly set values within the fragmentation tables or a species that is not correctly accounted for within the tables used.

Since its original development, this technique has so far proven to be a very powerful and versatile calculation method. Not only has it facilitated the calculation of ammonium, organic and other chemical concentrations, it also means that the evaluation of species can now be performed more thoroughly and systematically, and in a manner that is self-consistent across different AMS groups. This should mean that more accurate results can be obtained that are less prone to artefacts and chemical interferences. It has also allowed for the study of a multitude of other chemical types and sub-groups within types, such as studying different categories of organic groups such as polycyclic aromatic hydrocarbons, oxygenated and non-oxygenated hydrocarbons and markers for identifying biomass burning products. The details of these and the scientific conclusions arising will again be the subject of future publications.

While the example tables presented in this publication were current at the time of submission, work is continuously being performed by various groups within the worldwide AMS users community to update, expand and validate these tables, a process that is likely to be ongoing for some time. For the most recent fragmentation tables and information on the current work of the various groups, the reader is directed to http://cloudbase.phy.umist.ac.uk/people/allan/ja_igor.htm and http://cires.colorado.edu/jimenez/ams.html.

Acknowledgements

This work was supported by the UK Natural Environmental Research Council studentship NER/S/A/2000/03653 and grant GR3/12499. We thank the reviewers and editor for their helpful comments.

References

Alfarra, M. R., Coe, H., Allan, J. D., Bower, K. N., Boudries, H., Canagaratna, M. R., Jimenez, J. L., Jayne, J. T., Garforth, A., Li, S., & Worsnop, D. R. Characterization of urban and rural organic particulate in the lower Fraser Valley using two Aerodyne Aerosol Mass Spectrometers. *Atmospheric Environment*, in press.

Allan, J. D., Jimenez, J. L., Williams, P. I., Alfarra, M. R., Bower, K. N., Jayne, J. T., Coe, H., & Worsnop, D. R. (2003a). Quantitative sampling using an aerodyne aerosol mass spectrometer—1. Techniques of data interpretation and error analysis. *Journal of Geophysical Research-Atmosphere*, *108*, 4090.

Allan, J. D., Alfarra, M. R., Bower, K. N., Williams, P. I., Gallagher, M. W., Jimenez, J. L., McDonald, A. G., Nemitz, E., Canagaratna, M. R., Jayne, J. T., Coe, H., & Worsnop, D. R. (2003b). Quantitative sampling using an aerodyne aerosol mass spectrometer—2. Measurements of fine particulate chemical composition in two U.K. cities. *Journal of Geophysical Research-Atmosphere*, *108*, 4091.

Coplen, T. B., Bohlke, J. K., De Bievre, P., Ding, T., Holden, N. E., Hopple, J. A., Krouse, H. R., Lamberty, A., Peiser, H. S., Revesz, K., Rieder, S. E., Rosman, K. J. R., Roth, E., Taylor, P. D. P., Vocke, R. D., & Xiao, Y. K. (2002). Isotope-abundance variations of selected elements, IUPAC Technical report. *Pure and Applied Chemistry*, *74*, 1987–2017.

De Laeter, J. R., Bohlke, J. K., De Bievre, P., Hidaka, H., Peiser, H. S., Rosman, K. J. R., & Taylor, P. D. P. (2003). Atomic weights of the elements: Review 2000, IUPAC technical report. *Pure and Applied Chemistry*, *75*, 683–800.

Delia, A. E., Toohey, D., Canagaratna, M. R., Jimenez, J. L., Jayne, J. T., & Worsnop, D. R. Particulate ammonium from aerodyne aerosol mass spectrometer measurements, in preparation.

Jayne, J. T., Leard, D. C., Zhang, X. F., Davidovits, P., Smith, K. A., Kolb, C. E., & Worsnop, D. R. (2000). Development of an aerosol mass spectrometer for size and composition analysis of submicron particles. *Aerosol Science and Technology*, *33*, 49–70.

Jimenez, J. L., Jayne, J. T., Shi, Q., Kolb, C. E., Worsnop, D. R., Yourshaw, I., Seinfeld, J. H., Flagan, R. C., Zhang, X., Smith, K. A., Morris, J. W., & Davidovits, P. (2003). Ambient aerosol sampling using the aerodyne aerosol mass spectrometer. *Journal of Geophysical Research-Atmosphere*, *108*, 8425.

McLafferty, F. W., & Turecek, F. (1993). *Interpretation of mass spectra*. Mill Valley, CA: University Science Books.